Indonesian Journal of Pharmacy

VOL 36 (3) 2025: 545–556| RESEARCH ARTICLE

Nanoparticles Formulation of *Begonia medicinalis* Extract Using PLGA-Alginate-PVA Polymers for Immunomodulation and SARS-CoV-2 Protease Inhibition

Muhammad Sulaiman Zubair[1*], Reza Afriano[2],Ihwan Ihwan[1], Armini Syamsidi[1] and Evi Sulastri[1]

1. Department of Pharmacy, Faculty of Mathematics and Natural Sciences, Universitas Tadulako, Palu, Indonesia, 94118
2. Undergraduate Program of Pharmacy, Faculty of Mathematics and Natural Sciences, Universitas Tadulako, Palu, Indonesia, 94118

Article Info

Submitted: 11-02-2024
Revised: 21-12-2024
Accepted: 31-12-2024

*Muhammad Sulaiman Zubair

Email: sulaiman_zubair80@yahoo.co.id; sulaimanzubair@untad.ac.id

ABSTRACT

Begonia medicinalis herbs have been reported to have anticancer activity. In this research, nanoparticle delivery technology is applied to *Begonia medicinalis* herb extract to improve its effectiveness in medicine. This study aimed to investigate the physicochemical properties, and the potential immunomodulatory and anti-SARS-CoV-2 activities of nanoparticles formulated from *Begonia medicinalis* extract using a composite polymer of PLGA (Poly-Lactic-co-Glycolic Acid), sodium alginate (SA), and PVA (polyvinyl alcohol). Immunomodulatory effects were evaluated by measuring phagocytosis activity and levels of TNF-α and IFN-γ. Anti-SARS- CoV-2 activity was assessed via in vitro testing on the SARS-CoV-2 3CL protease enzyme. Nanoparticles were prepared using the solvent evaporation method with varying SA to PVA ratios (1:1, 1:2, 2:1, 2:2) designated as formulas 1, 2, 3, and 4. The nanoparticles were characterized by organoleptic examination, particle size measurement (179.3-250.7 nm), thermal degradation analysis at 190°C, and phytochemical content analysis. The total phenolic, flavonoid, and saponin contents ranged from 18.66-21.02 mg GAE/g, 1.86-2.49 mg QE/g, and 191.97-307.89 mg EE/g, respectively. The formulations showed significant immune-stimulating effects, including increased phagocytic activity and elevated TNF-α and IFN-γ levels. They also demonstrated inhibitory activity against the SARS-CoV-2 3CL protease enzyme. Encapsulation efficiency for phenolic, flavonoid, and saponin compounds ranged from 17-19%, 16-22%, and 60-96%, respectively. Among the formulations, nanoparticle formula 3 demonstrated the most favourable physicochemical properties. It exhibited strong immune-stimulating effects and significant inhibition of the SARS-CoV-2 virus, highlighting its potential for therapeutic application. In conclusion, *Begonia medicinalis* extract nanoparticles exhibit promising immunomodulatory effects and anti-SARS-CoV-2 activity underscoring their potential for therapeutic interventions against the virus.

Keywords: *Begonia medicinalis*, PLGA, Nanoparticles, Immunomodulation, Inhibition, SARS-CoV-2 Protease

INTRODUCTION

Begonia medicinalis herb, a traditional medicinal plant native to Central Sulawesi, has long been used to treat ailments such as asthma, gout, cancer, and tumors (Anam et al., 2014). Recent studies have highlighted its immunostimulatory potential, attributing this activity to the presence of notable saponin compounds, including 9(11)α, 16(17)α-dioxirane-20,25-dihydroxy-β-sitosterol-3-O-β-D glucopyranoside (Zubair et al., 2021; Zubair et al., 2022). However, the complex molecular structure of these saponins limits their ability to permeate biological membranes, underscoring the need to stabilize them within *B. medicinalis* formulations. Our previous research successfully developed a self-nanoemulsifying drug delivery system (SNEDDS) combining *B. medicinalis* and *Moringa oleifera* leaf extracts,

formulated with isopropyl myristate, tween 80, and propylene glycol. The resulting nanoparticles, with a size of 18.666 ± 0.208 nm, demonstrated good stability during storage (Asita et al., 2024). Building on this work, the current study explores the formulation of *B. medicinalis* using nanoparticle technology incorporating a composite polymer of (Poly-lactic-co-Glycolic Acid (PLGA), sodium alginate (SA), and polyvinyl alcohol (PVA).

One of the major challenges in herbal medicine is the limited penetration of extract compounds through the body's lipid membranes. Factors such as large molecular size and low water solubility reduce bioavailability and absorption (Ajazuddin & Saraf, 2010). Nanoparticle-based extract preparations offer a promising solution, with particle sizes typically ranging from 1 to 1000 nm (Dang & Guan, 2020; Strambeanu et al., 2015). Utilizing nanoparticle technology to develop *B. medicinalis* extract aims to enhance its stability and maximize its therapeutic potential. Polymers play a crucial role in nanoparticle formulation within the pharmaceutical field, enhancing drug stability, modifying characteristics, and enabling controlled release (Liechty et al., 2010). Composite polymers, which combine multiple polymers, are increasingly utilized to improve nanoparticle performance. This study focuses on fabricating novel nanoparticles of *B. medicinalis* extract using a blend of PLGA, SA, and PVA. PLGA is widely recognized for its biodegradability and FDA approval for therapeutic use in humans, demonstrating effectiveness in preserving phenolic content and bioactivity in extracts (Operti et al., 2021). It can be developed into polymeric nanoparticles through techniques such as emulsification-evaporation, nanoprecipitation, solvent displacement, solvent diffusion, and phase inversion, with particle sizes ranging from 10 to 1000 nm (Hernández-Giottonini, 2020). Alginate plays a pivotal role in drug delivery systems, encapsulating substances and integrating proteins into alginate-based nanoparticles and nanogels (Zhang et al., 2021). Known for its biocompatibility, biodegradability, and non-toxicity, alginate is widely used in the food and medical industries (Vijian et al., 2022).

Similarly, PVA, a water-soluble synthetic polymer, serves as an emulsion stabilizer and surface coating agent, as demonstrated in the production of rifaximin nanocomposites with PLGA (Takeuchi et al., 2021). PVA is also valued for its non-toxic nature, excellent biocompatibility, and good biodegradability (Rezagholizade-shirvan, et al., 2022; Afshar, et al., 2020). By combining these materials, the nanocomposite system is designed to effectively deliver *B. medicinalis* extract in nanoparticle form, facilitating its ability to penetrate cell membranes and enhance bioavailability. This study aims to formulate *B. medicinalis* extract nanoparticles utilizing PLGA/SA/PVA composite polymers, evaluate their physicochemical properties, and assess their immunomodulatory potential. By leveraging the unique attributes of these composite polymers, the research seeks to enhance nanoparticle performance while exploring their immunomodulatory effects.

MATERIALS AND METHODS

Sample Preparation

The leaves and stems of *B. medicinalis* were collected from Toddopoli village, Soyojaya district, North Morowali, Central Sulawesi, Indonesia. The plant species was authenticated by botanist Wisnu Ardi at the Bogor Botanical Gardens and registered under specimen number Wisnu Handoyo Ardi WI 447. Chemical reagents, including ethanol, SA, calcium chloride ($CaCl_2$), PVA, PLGA, chloroform, hydrochloric acid (HCl), sodium hydroxide (NaOH), gallic acid, Folin-Ciocalteau reagent, sodium carbonate (Na_2CO_3), escin, quercetin, potassium acetate (CH_3CO_2K), and aluminium chloride ($AlCl_3$) were sourced from Sigma Aldrich. The Untagged 3CL Protease Assay Kit was obtained from BPS Bioscience. The study adhered strictly to institutional review board guidelines outlined by the Ethics Committee for Medical and Health Research, Faculty of Medicine, Tadulako University, under the reference numbers 7918/UN28.1.30/KL/2020 and 1933/UN28.1.30/KL/2021. All experimental procedures complied with the specified ethical standards.

Sample preparation and Extraction.

The dried *B. medicinalis* simplicia was chopped with scissors and blended into a fine powder. The extraction was performed using 70% ethanol as the solvent at a ratio of 1:3. The powdered sample was macerated in the solvent for three days with daily stirring, followed by filtration. This maceration process was repeated three times, and the combined filtrates were evaporated to obtain a dense extract.

Nanoparticles Formulation of *B. medicinalis* extract

Nanoparticles were produced following Pin's method (Pin, 2015) with slight modifications.

Four formulations were prepared with varying SA-to-PVA ratios: 1:1, 1:2, 2:1, and 2:2 for formulas 1, 2, 3, and 4, respectively. A concentrated ethanol extract (180 mg) was dissolved in 1 mL of 70% ethanol and sonicated for 10 minutes in an ultrasonic bath (Eumax UD50SH 2L, 50 kHz). PLGA, dissolved in 5 mL of chloroform, was then added and sonicated for an additional 10 minutes with the addition of Span 60 to form Mixture A. Mixture A was combined with an SA solution (prepared by dissolving alginate in water and stirring at room temperature for 30 minutes) under vigorous stirring at approximately 600 rpm, resulting in Mixture B. Separately, PVA was dissolved in hot water, cooled, and mixed with a CaCl2 solution. Mixture B was then added dropwise into the PVA-CaCl2 blend under continuous stirring at high speed (±600 rpm). The final mixture was centrifuged at 5,000 rpm for 15 minutes at room temperature and freeze-dried to produce the nanoparticles.

Organoleptic Test.

This test aimed to evaluate the color, odor, and physical appearance of the *B. medicinalis* nanoparticles as part of their characterization (Annisa et al., 2023).

Particle Size and Zeta Potential Analysis.

The Particle Size Analysis (PSA) endeavors to quantify the dimensions of particles within the samples. This assessment used the Dynamic Light Scattering (DLS) method through the Malvern Zetasizer Instrument. To begin the analysis, we dispersed the powder sample in deionized water. We then transferred approximately 1 mL of this dispersion into a cuvette to measure the nanoparticle sizes (Babick, 2020).

Scanning Electron Microscopy.

Surface morphology analysis of the film was conducted using a Jeol JSM-IT300 with an operating voltage of 20 kV. SEM micrographs were obtained at magnifications of x100 and x5000, with distances ranging between 8.4 and 13.4 mm. Images were captured in three distinct areas of the sample to assess the uniformity and consistency of the nanostructures (Hodoroaba et al., 2016).

Thermal Gravimetric Analysis.

The thermal properties of the nanoparticles were assessed using a TGA instrument (TGA 4000, Perkin Elmer). Samples were heated to 600°C under experimental conditions. Each sample was positioned in an open platinum crucible, with an empty crucible serving as a reference. Thermal stability data were recorded at intervals of 10°C/minute (Chand & Vashishtha, 2000).

FT-IR Analysis.

FTIR spectroscopy (IR-Prestige-21, Shimadzu, Japan) was used to examine the infrared absorption characteristics of the nanoparticles. Samples were prepared in potassium bromide disks, and spectra were collected across wavenumbers ranging from 4000 cm^{-1} to 400 cm^{-1} at a resolution of 4 cm^{-1} (Warsito et al., 2017).

Total Phenolic Determination.

Ten mg of each nanoparticle sample was precisely weighed and treated with 1 M NaOH, followed by ten minutes in an ultrasonic bath (Eumax UD50SH 2L, 50 kHz) and heating in a water bath at 80°C for 10 minutes. The solution was then neutralized using 1 M HCl. A 1 mL portion of the resulting solution was combined with 0.4 mL of Folin-Ciocalteau reagent, mixed thoroughly, and left undisturbed for 4-8 minutes. The mixture was then supplemented with 4 mL of 7% Na_2CO_3 solution, thoroughly blended, and diluted to 10 mL with distilled water. After standing at room temperature for 2 hours, the sample's absorbance was measured using a UV-Vis spectrophotometer at 750.5 nm. Gallic acid (10-50 mg/L) was employed to construct the calibration curve (Sulastri et al., 2018).

Total Flavonoid Determination.

The nanoparticle sample (1 mL) was combined with 0.2 mL of 10% $AlCl_3$ in methanol, 0.2 mL of 1 M potassium acetate, and 5.6 mL of water. The mixture was incubated at room temperature for 30 minutes. The absorbance was then measured using a UV-Vis spectrophotometer at 433.5 nm. Quercetin (10-50 mg/L) was used as the standard for the calibration curve (Aryal et al., 2019).

Total Saponin Determination.

The nanoparticle solution (in 250 µL ethanol) was combined with 250 µL vanillin solution (8 g/100 mL ethanol) and 2.5 mL of 72% sulfuric acid. The mixture was heated at 60°C for 15 minutes, then cooled in cold water for 5 minutes.

The absorbance was measured at 599.5 nm using a UV-Vis spectrophotometer. Escin (Sigma Aldrich, 5-160 mg/L) was used as the standard for the calibration curve, with ethanol as the blank (Chua et al., 2019).

Entrapment Efficiency.

The entrapment efficiency was determined by comparing the total phenolic, flavonoid, and saponin concentrations in the formula to those in the original *B. medicinalis* extract using the following formula (Salatin et al., 2017) :

$$\%\ EE = \frac{Concentration\ in\ nanoparticle}{Concentration\ in\ extract} \times 100\%$$

Macrophage Phagocytosis Activity Test on Mice (*Mus musculus*).

The nanoparticles with the highest phenolic, saponin, and flavonoid concentrations were evaluated for phagocytosis activity and TNF-α and IFN-γ cytokine production. Male Balb/c mice (n = 4 per group) were acclimatized for 7 days with standard feed and water. The mice were divided into three treatment groups: Group 1 (negative control, 0.5% Na-CMC), Group 2 (positive control, Stimuno® 6.5 mg/kg BW), and Group 3 (nanoparticles, 60 mg/kg BW). Treatments were administered orally once daily for seven days. On day eight, each mouse received an intraperitoneal injection of 0.5 mL *Staphylococcus aureus* ATCC 25923 suspensions. After one hour, mice were anesthetized with ketamine (0.13 mg/mL) and their abdominal areas were surgically exposed. Peritoneal fluid was collected after gentle agitation with 1-2 mL sterile PBS (pH 7.8). Subsequently, 1 mL of peritoneal fluid was extracted, smeared on a glass slide, fixed with methanol (5 minutes), and stained with 10% Giemsa (20 minutes). After rinsing and air-drying, specimens were examined under oil immersion at 1000× magnification (Olympus CX23 LED). (Zubair et al., 2022). Phagocytic activity was calculated as:

$$\%Phagocityc\ activity = \frac{Number\ of\ active\ macrophages}{Number\ of\ observed\ macrophages} \times 100\%$$

TNF-α and IFN-γ Level Assay on Rats (*Rattus norvegicus*).

Wistar male rats were divided into three groups (n = 4 per group) and subjected to a seven-day treatment regimen: Group 1: Received 0.5% Na-CMC as the negative control. Group 2: Administered Stimuno® at a dose of 4.5 mg/kg BW as the positive control. Group 3: Treated with nanoparticles at a dose of 60 mg/kg BW.

On the eighth day, all animals were exposed to 0.3 mL of *Staphylococcus aureus* ATCC 25923 and allowed to incubate for one hour. Following this, surgical procedures were performed to collect blood samples directly from the heart into EDTA tubes. The collected blood was centrifuged (C2 Series®) at 3000 rpm for 15 minutes at room temperature to isolate plasma. Plasma samples were analyzed using an ELISA Reader (Elabscience®) according to the manufacturer's protocol (Zubair et al., 2022). Cytokine levels were quantified and expressed as picograms of cytokine per milliliter of protein.

Inhibition Percentage on SARS-CoV-2 3CL Assay.

Nanoparticles and *B. medicinalis* extract (20 mg) were dissolved in 0.2 mL of DMSO, from which 0.5 µL was mixed with 49.5 µL of 1 mM 1,4-dithio-D,L-threitol (DTT) to achieve a concentration of 1000 ppm. Subsequently, 10 µL of this solution was diluted to a final concentration of 200 ppm. The peptidomimetic GC376 was used as a positive control at a final concentration of 500 µM, prepared by diluting 50 µg in 200 µL of distilled water.

The assay procedure began with the addition of 30 µL of SARS-CoV-2 3CL protease enzyme, followed by preincubation at room temperature with gentle agitation for 30 minutes. Then, 10 µL of a fluorogenic substrate (DABCYL-KTSAVLQSGFRKME-EDANS) was added, and the mixture was incubated for 4 hours. Fluorescence intensity was measured at excitation/emission wavelengths of 360/460 nm using a Synergy HTX-3 Multi-mode Reader (Winooski, VT, USA) (Zubair et al., 2021).

Statistical analysis.

Results for TNF-α, IFN-γ, and SARS-CoV-2 3CL protease inhibition percentages were expressed as mean ± standard deviation (SD). One-way analysis of variance (ANOVA) was used for statistical comparisons between groups, followed by post hoc LSD testing. Statistical significance was set at $p < 0.05$, indicating significant differences between groups.

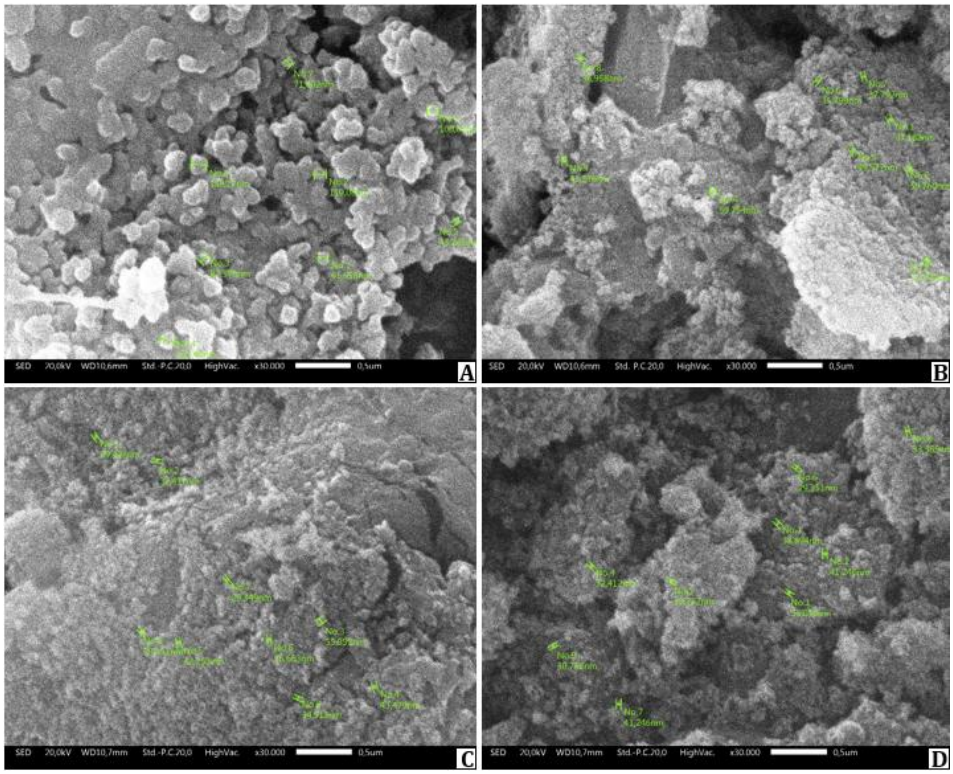

Figure 1. SEM images of (a) Nanoparticle 1, (b) Nanoparticle 2, (c) Nanoparticle 3, and (d) Nanoparticle 4, magnified at 30,000 x.

RESULTS AND DISCUSSION

Organoleptic, SEM, Particles size, polydispersity index (PDI), zeta potential (ZP), and Entrapment Efficiency.

The study utilized the solvent evaporation method to obtain nanoparticles, chosen for its efficiency and the ability to encapsulate drugs within a solution state, facilitating their integration into the nanoparticle drug delivery system (Hoa et al., 2012; Patra et al., 2018). Nanoparticle formation involved double emulsions created through single- or double-step processes. The single-step method was selected for its simplicity and spontaneous formation, despite yielding lower entrapment efficiency.

In the double-step method, the hydrophilic drug was dissolved in the aqueous phase, and PLGA was suspended in an appropriate organic solvent. The two phases were rigorously mixed to form a w/o emulsion. Subsequently, a second aqueous phase containing an emulsifier (PVA) was added to the w/o emulsion to create a double emulsion, followed by organic solvent evaporation. Nanoparticles were isolated using suitable absorbents or high-speed centrifugation with proper washing (Panigrahi et al., 2021). PLGA, approved by the FDA and EMA for drug delivery, stands out for its biocompatible and biodegradable properties (Han et al., 2016; Mir et al., 2017). Alginate, recognized for its biocompatibility, gel-forming capability, and adaptability to form nanoparticles, is widely used in drug delivery (Kirti & Khora, 2022). Similarly, PVA's biocompatibility, non-toxicity, and bioadhesive properties make it a key material for enhancing drug solubility and preparing solid dispersions (Gaaz et al., 2015; Rivera-Hernández et al., 2021).

Regarding organoleptic, SEM, and particle size analyses, no correlation was observed between various concentrations of alginate and PVA. The nanoparticles exhibited colours ranging from brown to white, emitting an odour akin to *B. medicinalis* extract. Morphologically, the nanoparticles displayed a spherical shape (Figure 1), but discrepancies in size were noted, leading to polydispersity, likely due to particle agglomeration driven by Brownian and Van Der Waals forces (Hernández-Giottonini et al., 2020).

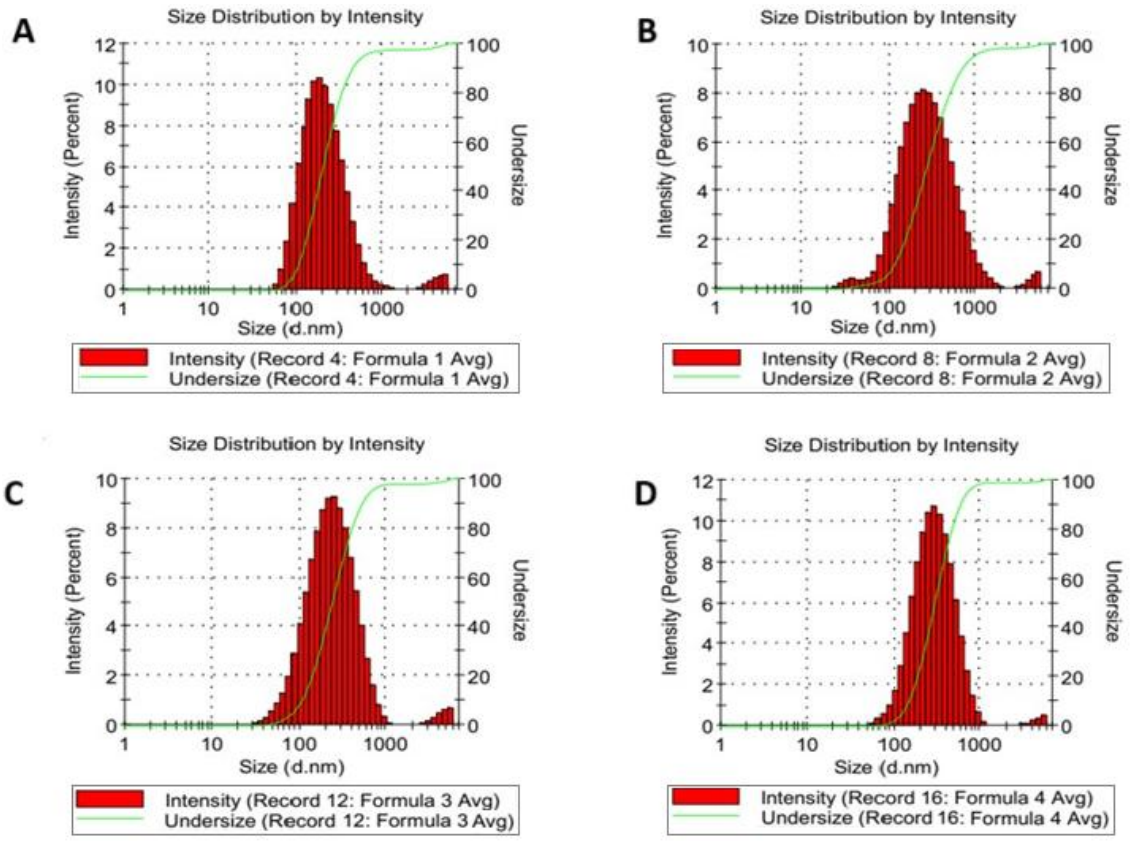

Figure 2. Size distribution analysis of (a) Nanoparticle 1, (b) Nanoparticle 2, (c) Nanoparticle 3, and (d) Nanoparticle 4

Particle size measurements ranged from 179.3 to 250.7 nm (Figure 2), consistent with previous research on PLGA nanoparticles (Mardiyanto, 2016). The polydispersity index (PDI) in the range 0,2657 to 0,2673. A small particle size and low PDI values can enhance the bioavailability of drugs (Shadab, et al., 2021), particularly in the case of *B. medicinalis* extract in this study. The PDI value are suggesting an ideal algorithm distribution (Robertson & Paul, 2000).

TGA and FTIR analysis

Thermogravimetric analysis (TGA) results (Figure 3a) revealed that formula 1 exhibited two-phase decomposition, mimicking the breakdown of organic material. The first phase occurred between 190°C and 370°C, followed by a second phase from 375°C to 545°C. Formulas 2, 3, and 4 demonstrated single-phase decomposition within 190°C–375°C. These results align with the decomposition behaviour of PLGA (Silva et al., 2015). Further research is necessary to fully understand the effects of heating nanoparticles within this range. Fourier-transform infrared spectroscopy (FTIR) analysis showed similar transmission peaks between the extract and nanoparticles, with an absorption band at 3400 cm^{-1} corresponding to hydroxyl (OH) groups. A shift in the OH group's wavenumber (from 3392 cm^{-1} to 3454–3512 cm^{-1}) indicated interactions between alginate and the extract. Additionally, a shift in the C=O group's wavenumber suggested interactions between the extract and PLGA (Figure 3b).

Phytochemical Content and Entrapment Efficiency.

Total phenolic, saponin, and flavonoid levels in the nanoparticles, expressed as gallic acid equivalents per gram (GAE/g), escin equivalents per gram (EE/g), and quercetin equivalents per gram (QE), respectively (Table I). Comparative analysis with the ethanol extract revealed differences in concentrations between the extract and the formulated nanoparticles.

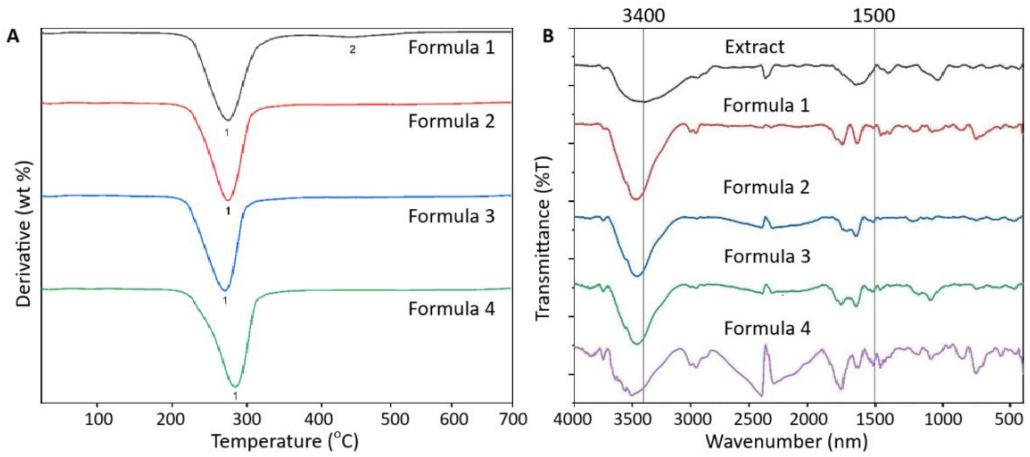

Figure 3. a) TGA spectra of *B. medicinalis* nanoparticle; b) FTIR spectra of 70% ethanol extract and nanoparticle of *B. medicinalis*.

Table I. Phytochemistry Content of Nanoparticle Formula (mean ± SD, n = 3)

Formulation	Total phenolic (mg GAE/g)	Total saponin (mg EE/g)	Total flavonoid (mg QE/g)
Nanoparticle 1	19.69± 2.19	191.97 ± 74.82	1.97 ± 0.06
Nanoparticle 2	20.46 ± 1.84	247.61 ± 78.38	1.86 ± 0.10
Nanoparticle 3	21.02 ± 2.67	307.89 ± 44.84	2.49 ± 0.21
Nanoparticle 4	18.66 ± 1.01	229.00 ± 52.03	2.21 ± 0.46

mg GAE/g: milligrams of gallic acid equivalents per gram; mgEE/g: milligrams of escin equivalents per gram; mgQE/g: milligrams of quercetin equivalents per gram

Table II. The Efficiency Entrapment of Nanoparticle Formula

Formulation	Entrapment efficiency for phenolic compound (%)	Entrapment efficiency for saponin compound (%)	Entrapment efficiency for flavonoid compound (%)
Nanoparticle 1	17 ± 1	60 ± 23	17 ± 1
Nanoparticle 2	18 ± 1	77 ± 16	16 ± 1
Nanoparticle 3	19 ± 3	96 ± 31	22 ± 2
Nanoparticle 4	17 ± 1	71 ± 21	19 ± 4

The average phenolic concentration in the nanoparticles ranged from 18.66 to 21.03 mg GAE/g, significantly lower than the extract (112.02 mg GAE/g). Similarly, flavonoid levels in the nanoparticles (1.86 to 2.49 mg QE/g) were much lower than in the extract (11.35 mg QE/g). In contrast, saponin content in nanoparticle 3 (307.89 mg EE/g) was comparable to the extract (319.72 mg EE/g) (Zubair et al., 2022). Variations in phenolic, saponin, and flavonoid contents were influenced by the PVA/alginate ratio, with nanoparticle 3 exhibiting the highest phytochemical content among the formulations. Particle size and entrapment efficiency analysis (Table II) revealed no correlation between alginate and PVA concentrations in the formulations. This aligns with the findings of Takeuchi et al., (2021), which reported that PVA concentration had no significant effect on Rifaximin content within nanoparticles.

Effect of nanoparticles on production of macrophage phagocytosis, TNF-α, IFN-γ and inhibition percentage on SARS-CoV-2 3CL.

After seven days of nanoparticle administration, macrophage phagocytosis activity was significantly enhanced compared to both positive and negative controls (Figure 4a).

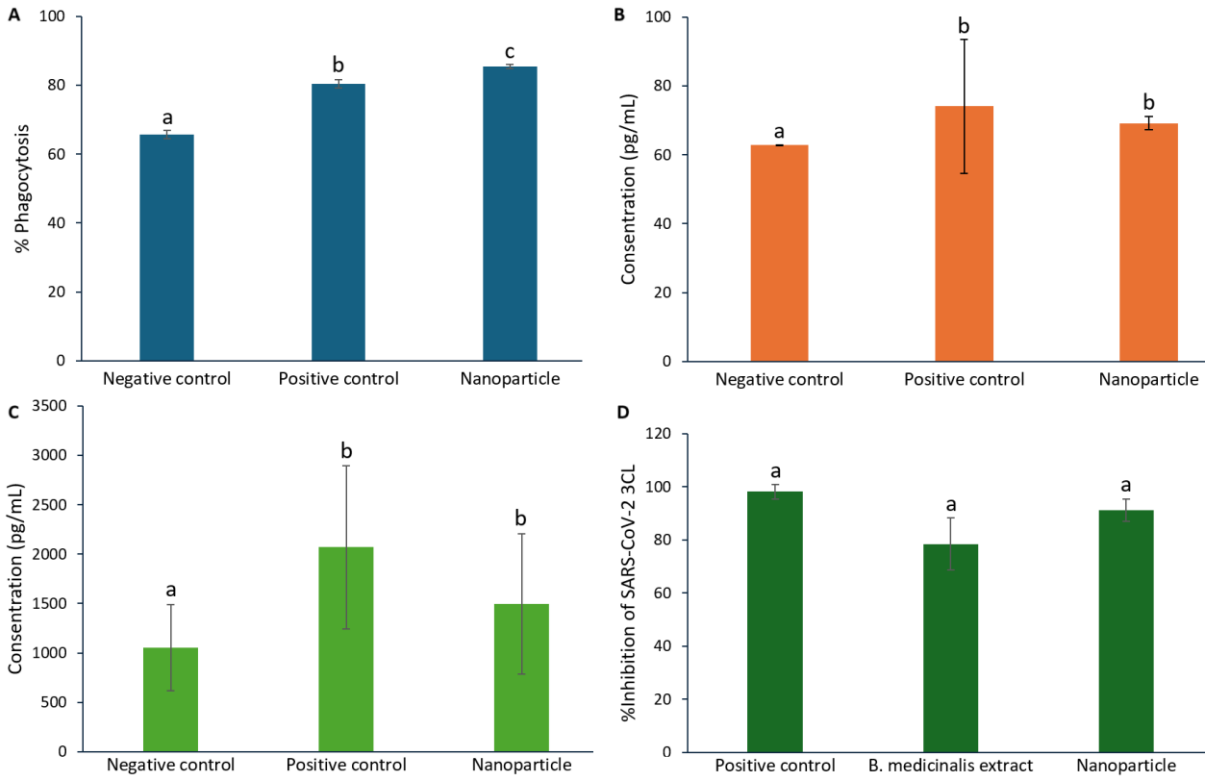

Figure 4. Effect of nanoparticles 3 of *B. medicinalis* on production of a) Macrophage phagocytosis, b) TNF-α, c) IFN-γ, and d) Inhibition percentage of SARS-CoV-2 3C enzyme. The different letter superscript means significant difference by post hoc LSD test at $p<0.05$).

In terms of TNF-α levels (Figure 4b), nanoparticles showed an average concentration of 1496.67±710.23 pg/mL, slightly lower than the positive control (2070±828.19 pg/mL) but significantly higher than the negative control (1056.67±435.47 pg/mL, $p < 0.05$). This indicates the immunomodulatory potential of the nanoparticles.

Similarly, IFN-γ levels (Figure 4c) in the nanoparticle-treated group (69.19±1.94 pg/mL) were marginally lower than the positive control (74.07±19.52 pg/mL) and significantly higher than the negative control (62.78±0.02 pg/mL, $p < 0.05$). These findings further support the immunomodulatory properties of the nanoparticles.

Flavonoid compounds are known to exhibit immunostimulatory properties by promoting the macrophage and lymphocyte proliferation. The immunomodulatory mechanism of flavonoids involves the upregulation of IL-12 activity and the promotion of lymphocyte proliferation. This increased population of T lymphocytes stimulates macrophage activation, leading to enhanced cytokine secretion, including IL-1, IL-6, IL-12, and TNF-α. This cascade amplifies bacterial phagocytosis by macrophages. TNF-α plays a pivotal role in the acute inflammatory response to Gram-negative bacteria and other microbes. During severe infections, substantial TNF levels may induce systemic responses. The primary producers of TNF-α include mononuclear phagocytes, antigen-activated T cells, NK cells, and mast cells. Lipopolysaccharides serve as potent stimuli for macrophage TNF secretion. Similarly, IFN-γ, produced by T cells and NK cells, stimulates macrophages by enhancing TNF synthesis and other immunomodulatory functions (López-García & Castro-Manrreza, 2021).

Inhibition Percentage on SARS-CoV-2 3CL

The in vitro enzymatic activity assay (Figure 4d) employing the fluorescence energy transfer (FRET) method, revealed that nanoparticles exhibited the highest inhibitory activity (91.19 % ± 4.12), closely matching the positive control (98.19

% ± 2.72). In comparison, the percent inhibition for *B. medicinalis* extract alone was lower (78.50 % ± 9.88) but not significantly different from either sample ($p>0.05$). These findings emphasize the enhanced effectiveness of *B. medicinalis* extract when formulated into nanoparticles for enzyme inhibition.

Active compounds identified in *B. medicinalis* include flavonoids, phenolics, saponins, and terpenoids/steroids (Zubair, et al., 2021; Zubair et al., 2022; Zubair et al., 2021). The inhibitory activity of *B. medicinalis* against the SARS-CoV-2 3CL protease enzyme aligns with previous reports highlighting the role of terpenoid compounds such as β-sitosterol in inhibiting SARS-CoV 3CL protease with an IC_{50} of 1210 μM (Lin et al., 2005). Terpenoid compounds such as 24-methylcholesta-7en-3β-on also demonstrate 76% inhibition of SARS-CoV-2 3CL protease activity at a concentration of 200 ppm (Zubair et al., 2021). These findings underscore the *B. medicinalis* as a promising candidate for COVID-19 treatment.

CONCLUSION

Nanoparticles containing *B. medicinalis* extract were successfully formulated using a composite polymer of PLGA, SA, and PVA, the particle sizes ranging from 179.3 to 250 nm and maintaining a spherical morphology. Among tested formulations, Formula 3 (SA:PVA ratio of 2:1) emerged as the best formulation, exhibiting superior characteristics and favourable properties. It demonstrated high levels of total phenolic, flavonoid, and saponin content alongside optimal entrapment efficiency. In vivo testing highlighted its remarkable ability to stimulate an immune response, evidenced by increased macrophage phagocytosis and elevated TNF-α/IFN-γ levels. The heightened immunomodulatory activity suggests its potential application in strategies for treating SARS-CoV-2. These promising results offer prospects for further exploration and development of *B. medicinalis* nanoparticles in the field of infectious viral disease treatment.

ACKNOWLEDGMENTS

This research was financially supported by The General Directorate of Higher Education, Research and Technology, The Ministry of Education, Culture, Research and Technology, Republic of Indonesia, through National Competitive Applied Research Grant with the contract number 918a/UN28.2/PL/2021.

CONFLICT OF INTEREST

The authors declare no conflict of interest.

REFERENCES

Ajazuddin, & Saraf, S. (2010). Applications of novel drug delivery system for herbal formulations. *Fitoterapia*, *81*(7), 680–689. https://doi.org/10.1016/j.fitote.2010.05.001

Anam, S., Ritna, A., Dwimurti, F., Rismayanti, D., & Zubair, M. S. (2014). Cytotoxic activity of methanol extract of benalu batu (Begonia sp.): Ethnomedicine of the Wana tribe of Central Sulawesi. *Jurnal Ilmu Kefarmasian Indonesia*, *12*(1), 10–16.

Annisa, R., Fauziyah, B., Megawati, D. S., & Zahrah, F. (2023). Formulation of silver nanoparticle mouthwash and testing of antibacterial activity against Staphylococcus aureus. *Journal of Tropical Pharmacy and Chemistry*, *7*(2), 52–58. https://doi.org/10.25026/jtpc.v7i2.386

Anonim. (2012). *Nanocomposix's guide to dynamic light scattering measurement and analysis*. Nanocomposix's.

Aryal, S., Baniya, M. K., Danekhu, K., Kunwar, P., Gurung, R., & Koirala, N. (2019). Total phenolic content, flavonoid content and antioxidant potential of wild vegetables from Western Nepal. *Plants*, *8*(4), 96. https://doi.org/10.3390/plants8040096

Asita, N., Zubair, M. S., Syukri, Y., & Sulastri, E. (2024). Formulation of Self-Nanoemulsifying Drug Delivery System (SNEDDS) Formula of Combined 70% Ethanolic of B. medicinalis Herbs and M. oleifera Leaves. *Pharmacy Education Journal*, *24*(3), 304–309. https://doi.org/10.46542/pe.2024.243.304309

Afshar, M., Dini, G., Vaezifar, S., Mehdikhani, M., & Movahedi, B. (2020). Preparation and characterization of sodium alginate/polyvinyl alcohol hydrogel containing drug-loaded chitosan nanoparticles as a drug delivery system. *Journal of Drug Delivery Science and Technology*, *56*, 101530.

Babick, F. (2020). Dynamic light scattering (DLS). In *Characterization of nanoparticles* (pp. 137–172). Elsevier. https://doi.org/10.1016/B978-0-12-814182-3.00010-9

Chand, N., & Vashishtha, S. R. (2000). Development, structure and strength properties of PP/PMMA/FA blends. *Bulletin of Materials Science*, *23*(2), 103–107. https://doi.org/10.1007/BF02706550

Chua, L. S., Lau, C. H., Chew, C. Y., & Dawood, D. A. S. (2019). Solvent fractionation and acetone precipitation for crude saponins from Eurycoma longifolia extract. *Molecules*, *24*(7), 1416. https://doi.org/10.3390/molecules24071416

Dang, Y., & Guan, J. (2020). Nanoparticle-based drug delivery systems for cancer therapy. *Smart Materials in Medicine*, *1*, 10–19. https://doi.org/10.1016/j.smaim.2020.04.001

Gaaz, T., Sulong, A., Akhtar, M., Kadhum, A., Mohamad, A., & Al-Amiery, A. (2015). Properties and applications of polyvinyl alcohol, halloysite nanotubes and their nanocomposites. *Molecules*, *20*(12), 22833–22847. https://doi.org/10.3390/molecules201219884

Han, F. Y., Thurecht, K. J., Whittaker, A. K., & Smith, M. T. (2016). Bioerodable PLGA-based microparticles for producing sustained-release drug formulations and strategies for improving drug loading. *Frontiers in Pharmacology*, *7*. https://doi.org/10.3389/fphar.2016.00185

Hernández-Giottonini, K. Y., Rodríguez-Córdova, R. J., Gutiérrez-Valenzuela, C. A., Peñuñuri-Miranda, O., Zavala-Rivera, P., Guerrero-Germán, P., & Lucero-Acuña, A. (2020). PLGA nanoparticle preparations by emulsification and nanoprecipitation techniques: Effects of formulation parameters. *RSC Advances*, *10*(8), 4218–4231. https://doi.org/10.1039/C9RA10857B

Hoa, L. T. M., Chi, N. T., Nguyen, L. H., & Chien, D. M. (2012). Preparation and characterisation of nanoparticles containing ketoprofen and acrylic polymers prepared by emulsion solvent evaporation method. *Journal of Experimental Nanoscience*, *7*(2), 189–197. https://doi.org/10.1080/17458080.2010.515247

Hodoroaba, V.-D., Rades, S., Salge, T., Mielke, J., Ortel, E., & Schmidt, R. (2016). Characterisation of nanoparticles by means of high-resolution SEM/EDS in transmission mode. *IOP Conference Series: Materials Science and Engineering*, *109*, 012006. https://doi.org/10.1088/1757-899X/109/1/012006

Kirti, & Khora, S. S. (2022). Alginate: A promising biopolymer in drug delivery system. In S. Jana & S. Jana (Eds.), *Marine Biomaterials* (pp. 61–95). Springer Nature Singapore. https://doi.org/10.1007/978-981-16-4787-1_3

Liechty, W. B., Kryscio, D. R., Slaughter, B. V., & Peppas, N. A. (2010). Polymers for drug delivery systems. *Annual Review of Chemical and Biomolecular Engineering*, *1*, 149–173. https://doi.org/10.1146/annurev-chembioeng-073009-100847

Lim, M. P. (2015). *Core-shell structure alginate-PLGA/PLLA microparticles as a novel drug delivery system for water soluble drugs* [Nanyang Technological University]. https://doi.org/10.32657/10356/62178

Lin, C.-W., Tsai, F.-J., Tsai, C.-H., Lai, C.-C., Wan, L., Ho, T.-Y., Hsieh, C.-C., & Chao, P.-D. L. (2005). Anti-SARS coronavirus 3C-like protease effects of Isatis indigotica root and plant-derived phenolic compounds. *Antiviral Research*, *68*(1), 36–42. https://doi.org/10.1016/j.antiviral.2005.07.002

López-García, L., & Castro-Manrreza, M. E. (2021). TNF-α and IFN-γ Participate in Improving the Immunoregulatory Capacity of Mesenchymal Stem/Stromal Cells: Importance of Cell-Cell Contact and Extracellular Vesicles. *International Journal of Molecular Sciences*, *22*(17), 9531. https://doi.org/10.3390/ijms22179531

Mardiyanto. (2016). Preparation and characterization of submicron particles of PLGA incorporating rifampin using emulsion solvent diffusion. *Proceeding - ICB Pharma II "Current Breakthrough in Pharmacy Materials and Analyses."*

Mir, M., Ahmed, N., & Rehman, A. U. (2017). Recent applications of PLGA based nanostructures in drug delivery. *Colloids and Surfaces B: Biointerfaces*, *159*, 217–231. https://doi.org/10.1016/j.colsurfb.2017.07.038

Operti, M. C., Bernhardt, A., Grimm, S., Engel, A., Figdor, C. G., & Tagit, O. (2021). PLGA-based nanomedicines manufacturing: Technologies overview and challenges in industrial scale-up. *International Journal of Pharmaceutics*, *605*, 120807.

https://doi.org/10.1016/j.ijpharm.2021.120807

Panigrahi, D., Sahu, P. K., Swain, S., & Verma, R. K. (2021). Quality by design prospects of pharmaceuticals application of double emulsion method for PLGA loaded nanoparticles. *SN Applied Sciences*, *3*(6), 638. https://doi.org/10.1007/s42452-021-04609-1

Patra, J. K., Das, G., Fraceto, L. F., Campos, E. V. R., Rodriguez-Torres, M. D. P., Acosta-Torres, L. S., Diaz-Torres, L. A., Grillo, R., Swamy, M. K., Sharma, S., Habtemariam, S., & Shin, H.-S. (2018). Nano based drug delivery systems: Recent developments and future prospects. *Journal of Nanobiotechnology*, *16*(1), 71. https://doi.org/10.1186/s12951-018-0392-8

Rezagholizade-shirvan, A., Najafi, M. F., Behmadi, H., & Masrournia, M. (2022). Preparation of nano-composites based on curcumin/chitosan-PVA-alginate to improve stability, antioxidant, antibacterial and anticancer activity of curcumin. *Inorganic Chemistry Communications*, *145*, 110022.

Rivera-Hernández, G., Antunes-Ricardo, M., Martínez-Morales, P., & Sánchez, M. L. (2021). Polyvinyl alcohol based-drug delivery systems for cancer treatment. *International Journal of Pharmaceutics*, *600*, 120478. https://doi.org/10.1016/j.ijpharm.2021.120478

Robertson, G. P., & Paul, E. A. (2000). Decomposition and soil organic matter dynamics. In O. E. Sala, R. B. Jackson, H. A. Mooney, & R. W. Howarth (Eds.), *Methods in Ecosystem Science* (pp. 104–116). Springer New York. https://doi.org/10.1007/978-1-4612-1224-9_8

Salatin, S., Barar, J., Barzegar-Jalali, M., Adibkia, K., Kiafar, F., & Jelvehgari, M. (2017). Development of a nanoprecipitation method for the entrapment of a very water soluble drug into eudragit RL nanoparticles. *Research in Pharmaceutical Sciences*, *12*(1), 1–14. https://doi.org/10.4103/1735-5362.199041

Silva, M. F., Hechenleitner, A. A. W., Irache, J. M., Oliveira, A. J. A. D., & Pineda, E. A. G. (2015). Study of thermal degradation of PLGA, PLGA nanospheres and PLGA/maghemite superparamagnetic nanospheres. *Materials Research*, *18*(6), 1400–1406. https://doi.org/10.1590/1516-1439.045415

Strambeanu, N., Demetrovici, L., Dragos, D., & Lungu, M. (2015). Nanoparticles: Definition, classification and general physical properties. In M. Lungu, A. Neculae, M. Bunoiu, & C. Biris (Eds.), *Nanoparticles' Promises and Risks* (pp. 3–8). Springer International Publishing. https://doi.org/10.1007/978-3-319-11728-7_1

Sulastri, E., Zubair, M. S., Anas, N. I., Abidin, S., Hardani, R., Yulianti, R., & Aliyah A, A. (2018). Total phenolic, total flavonoid, quercetin content and antioxidant activity of standardized extract of Moringa oleifera leaf from regions with different elevation. *Pharmacognosy Journal*, *10*(6s), s104–s108. https://doi.org/10.5530/pj.2018.6s.20

Shadap, Md., Alhakamy, N. A., Neamatallah, T., Alshehri, S., Mujtaba, M. A., Riadi, Y., ... & Akhter, M. H. (2021). Development, characterization, and evaluation of α-Mangostin-loaded polymeric nanoparticle gel for topical therapy in skin Cancer. Gels, 7(4), 230.

Takeuchi, I., Kato, Y., & Makino, K. (2021). Effects of polyvinyl alcohol on drug release from nanocomposite particles using poly (L-lactide-*co*-glycolide). *Journal of Oleo Science*, *70*(3), 341–348. https://doi.org/10.5650/jos.ess20299

Vijian, R. S., Yusefi, M., & Shameli, K. (2022). Plant extract loaded sodium alginate nanocomposites for biomedical applications: A review. *Journal of Research in Nanoscience and Nanotechnology*, *6*(1), 14-30.

Warsito, W., Noorhamdani, N., Sukardi, S., & Dwi Susanti, R. (2017). Microencapsulation of Cytrus hystrix oil and its activity test as an antimicrobial agent. *Journal of Enviromental Engineering and Sustainable Technology*, *4*(2), 131–137. https://doi.org/10.21776/ub.jeest.2017.004.02.9

Zhang, H., Cheng, J., & Ao, Q. (2021). Preparation of alginate-based biomaterials and their applications in biomedicine. *Marine Drugs*, *19*(5), 264. https://doi.org/10.3390/md19050264

Zubair, M., Maulana, S., Widodo, A., Pitopang, R., Arba, M., & Hariono, M. (2021). GC-MS, LC-

MS/MS, docking and molecular dynamics approaches to identify potential SARS-CoV-2 3-chymotrypsin-like protease inhibitors from Zingiber officinale Roscoe. *Molecules*, *26*(17), 5230. https://doi.org/10.3390/molecules26175230

Zubair, M. S., Alarif, W. M., Ghandourah, M. A., & Anam, S. (2021). A new steroid glycoside from *Begonia sp.*: Cytotoxic activity and docking studies. *Natural Product Research*, *35*(13), 2224–2231. https://doi.org/10.1080/14786419.2019.1669026

Zubair, M. S., Khairunisa, S. Q., Sulastri, E., Ihwan, Widodo, A., Nasronudin, & Pitopang, R. (2021). Antioxidant and antiviral potency of Begonia medicinalis fractions. *Journal of Basic and Clinical Physiology and Pharmacology*, *32*(4), 845–851. https://doi.org/10.1515/jbcpp-2020-0476

Zubair, M. S., Syamsidi, A., Sulastri, E., Widyasari, N., Sanjaya, I. P., & Pakaya, D. (2022). Immunomodulatory activity of benalu batu (Begonia medicinalis) ethanolic extract in experimental animals. *Indonesian Journal of Pharmacy*, *33*(4), 575–582. https://doi.org/doi.org/10.22146/ijp.3588